2002 HST Calibration Workshop
Space Telescope Science Institute, 2002
S. Arribas, A. Koekemoer, and B. Whitmore, eds.

STIS Status after the Switch to Side 2

Thomas M. Brown and James E. Davies

Space Telescope Science Institute, Baltimore, MD 21218

Abstract.

Since July 2001, STIS has been operating on its secondary (Side-2) electronics, due to the failure of the primary (Side-1) system. The change to Side 2 has required new calibration work. The dark rate of the STIS CCD varies since the switch to Side 2, as it depends on the temperature of the CCD (which cannot be regulated precisely using Side-2 electronics). We find that the dark rate is a linear function of the housing temperature for pixels at a given dark rate, but the slope of this relation varies for pixels with different dark rates. Scaling of the darks as a function of the temperature has been incorporated into the STIS pipeline. An additional feature of the switch to Side-2 is that the STIS CCD read noise has increased by 1 e^- sec^{-1} for all four amplifiers when using a gain of 1. This increased read noise is due to electronic pick-up pattern noise (on Side 1 the noise was primarily white noise). Although an algorithm exists for filtering this additional pattern noise, it will not be incorporated into the STIS pipeline.

1. Introduction

The Space Telescope Imaging Spectrograph (STIS) was launched in 1997 with two sets of redundant electronics, but a unique set of detectors. The sets of electronics are referred to as "Side 1" and "Side 2." STIS ran on its Side-1 electronics until May of 2001, at which point the instrument safed due to catastrophic failure of these electronics. After an extended period of testing, it was determined that the Side-1 electronics were unrecoverable; they are also not designed for repair during the servicing missions. Thus, STIS operations were resumed with the Side-2 electronics in July of 2001. STIS performance did not change significantly in the switch from Side 1 to Side 2, except that the CCD read noise has moderately increased, and the loss of CCD temperature control produces a variable dark rate. We summarize these changes here; they are discussed more fully by Brown (2001a, 2001b).

2. Dark Rate Variations with Temperature

On Side 1, a temperature sensor mounted on the CCD carrier provided closed-loop control of the current provided to the thermoelectric cooler (TEC), thus ensuring a stable detector temperature at the commanded set point (-83^oC). Side 2 does not have a functioning temperature sensor, so the TEC is run at a constant current. Thus, under Side-2 operations, the CCD temperature varies with that of the spacecraft environment. Although no sensor is available to measure the temperature of the CCD itself, there is a sensor for the CCD housing temperature, which should track closely with the detector temperature under Side-2 operations (but not for Side-1). This housing temperature is reported in STIS CCD science headers under the keyword OCCDHTAV; note that it is far hotter than the detector itself (the housing is typically near 18^oC while the detector runs near -83^oC).

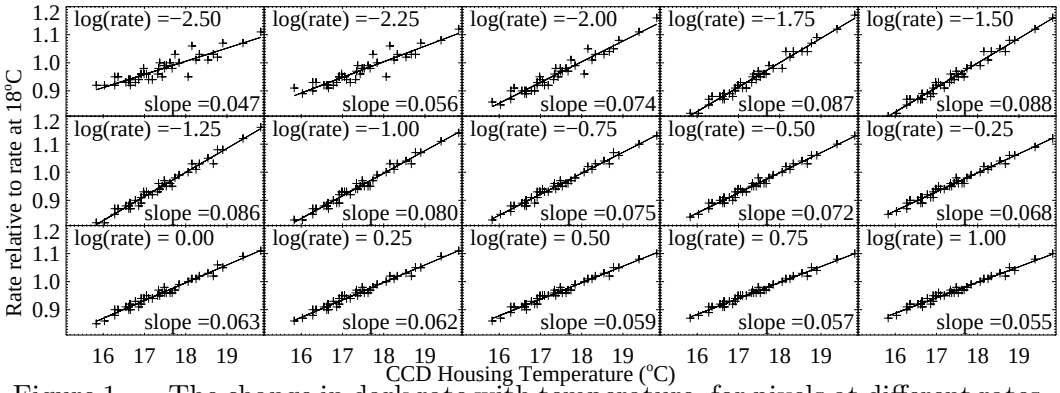

Figure 1. The change in dark rate with temperature, for pixels at different rates. The change in dark rate is linear for pixels at a given rate, but the slope of this linear relation depends on the rate in question.

Because the dark rate for the STIS CCD is strongly temperature dependent, the dark rate is now much more variable in CCD observations (compared to observations on Side-1). The relation is linear for pixels at a given dark rate (Figure 1), but the increase with temperature varies from $\sim$ 5%–9% for every °C, depending upon the rate of a particular pixel. Pixels with low dark rates will vary by $\sim$ 5% per °C, pixels with moderately high dark rates will vary by $\sim$ 9% per °C, and the pixels with the highest dark rates will vary by $\sim$ 6% per °C.

This variable dark rate presents a problem for calibration, as the temperature can vary between one science exposure and the next, and between one dark exposure and the next. For accurate subtraction of the dark current, the temperature dependence of the dark rate must be included in the pipeline processing of the raw data.

To this end, a new header keyword OCCDHTAV giving the CCD housing temperature has been added to the STIS science headers. A simplified scheme that assumes a dark rate variation of 7% per °C for all pixels has been implemented into the STSDAS calstis software and the archive On The Fly Reprocessing (OTFR) software. Calibration dark files are created so that they reproduce the dark at a housing temperature of 18°C, and then are scaled up or down to match the temperature of a given science frame prior to dark subtraction. The new dark subtraction algorithm for processing Side-2 CCD data came into use in January 2002. Note that more complicated schemes for subtracting the dark current (which use the pixel-to-pixel variation in dark rate with temperature) show little improvement over this simplified scheme, mainly due to the poor statistics in characterizing individual pixels in a given time period.

Side-1 data retrieved from the archive should have a negative value for OCCDHTAV (indicating to the software that it should not be used for scaling the dark subtraction). Unfortunately, when the temperature-dependent dark subtraction was implemented, a bug in the software used only the year of the observations to determine if the data were taken on Side 1 or Side 2, and thus the first 5 months of 2001 were treated as Side-2 data and given a positive (and meaningless) OCCDHTAV value. This bug was fixed with the archive software update of September 2002. Thus, any observations taken from January to May in 2001, but retrieved from the archive in January to August of 2002, will have an incorrect dark subtraction, and should be re-retrieved from the archive with OTFR.

3. Increased Read Noise

CCD data taken using Side 2 show an increase in effective read noise of approximately 1 e^- pix^{-1} for gain = 1 and 0.2 e^- pix^{-1} for gain = 4. This elevated read noise manifests

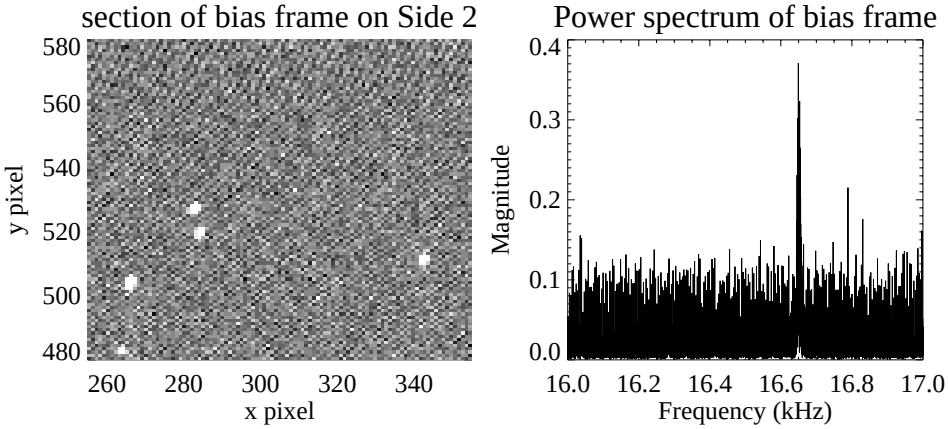

Figure 2. *Left panel:* A section of a raw CCD bias frame. Notice the herring-bone pattern noise. *Right panel:* A Fourier transform of the 1-D time series (as it was read out in the Side-2 electronics) of the same bias frame. There is a peak in the power spectrum at 16.65 kHz, which corresponds to a horizontal pattern with 2.73 pixel spacing on the CCD.

itself as a herring-bone pattern that can be seen easily on a short exposure such as a raw bias frame (Figure 2). When the 2-D image is converted to a 1-D time series (using the timing intervals for clocking out the CCD), a Fourier transform of the series indicates that the read noise pattern is temporally correlated. In this example, there is a peak in the power spectrum at about 16.65 kHz. Pipeline-processed CCD data also show this pattern noise. In fact, the pattern noise is usually much more apparent in processed, cosmic-ray-rejected images than it is in the raw, unprocessed images.

The frequency of the pattern noise is typically 15.5–18 kHz. There is a correlation between the pattern noise frequency and the CCD housing temperature, but the correlation is too loose to be useful for predicting the frequency accurately enough to assist with filtering (see below). Timing frequencies in this range correspond to a spatial frequency of approximately 3 pixels on the detector (horizontally, in the direction of serial clocking).

STIS CCD images and spectral images can sometimes be filtered by interpolating the power spectrum to remove the peak from the pattern noise. We have provided an IDL script to analyze the pattern noise and attempt filtering, at
ftp://ftp.stsci.edu/pub/instruments/stis/stisnoise.pro.
This noise removal will not be added to the archive pipeline; the current procedure requires careful tuning of the filter position and width in Fourier space, which requires user interaction and evaluation of the results. Also, the filter often introduces undesirable artifacts into the data, which must be weighed against the advantages of filtering on a case-by-case basis. As the width of the filter is decreased, the artifacts decrease, but at some point some of the pattern noise escapes the filter (due to the frequency wandering across the image). The best filter width is typically about 20 Hz. Note that our software uses a fairly primitive filtering method; we would appreciate any feedback on superior filtering techniques that have been shown to work with the STIS pattern noise.

Figures 3 and 4 show two examples of data filtered with the IDL routine provided: the crowded star field of 47 Tuc and the diffuse galaxy UGC 2847. These examples represent the two extremes encountered in filtering. Images crowded with point sources tend to suffer the most artifacts, while images with diffuse sources tend to filter well.

Acknowledgments. We are grateful to L. Dressel, R. Allen, P. Goudfrooij, R. Kimble, and T. Gull for their insight and useful discussions.

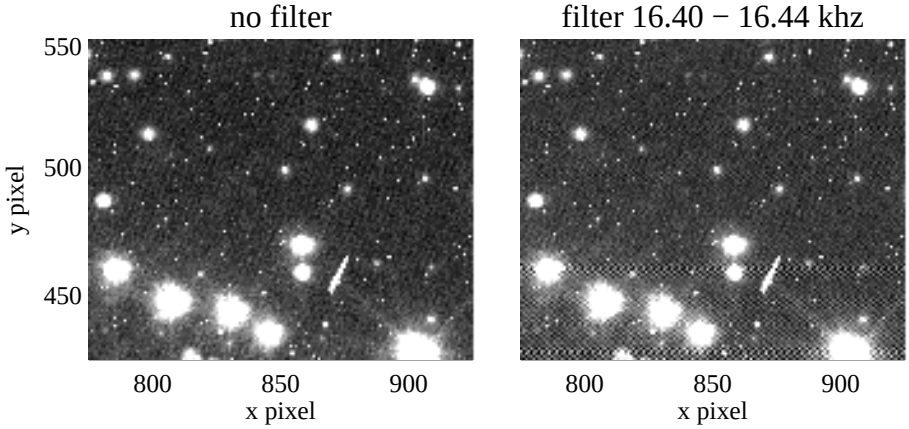

Figure 3. A crowded star field in 47 Tuc, before (*left*) and after (*right*) filtering. This is an example of data that cannot be filtered with the current algorithm. The power spectrum did not reveal the pattern noise frequency, and a narrow filter introduces artifacts around the bright stars.

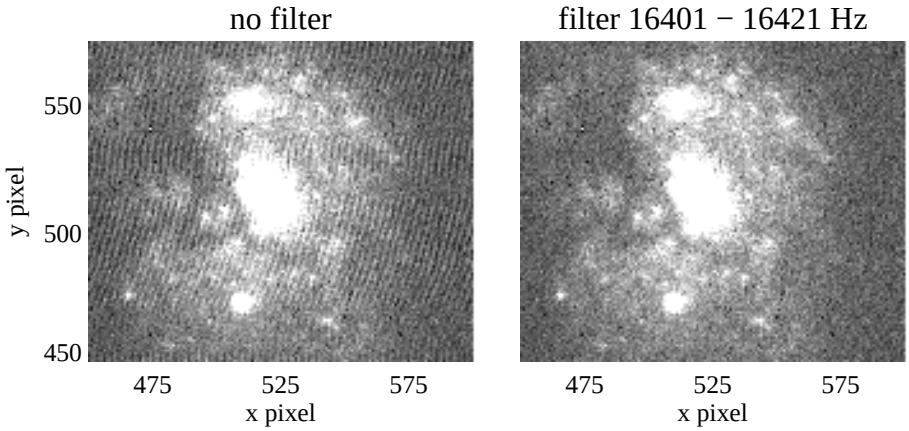

Figure 4. *Left panel:* An image section of UGC 2847. The pattern noise is very striking in this short exposure, and makes it difficult to see the galactic structure. *Right panel:* Application of a narrow filter completely removes the pattern noise without introducing artifacts. Filtering works best in sparse, faint, diffuse images.

References

Brown, T. M. 2001a, "Temperature Dependence of the STIS CCD Dark Rate During Side-2 Operations", *Instrument Science Report* STIS 2001-03 (Baltimore: STScI)

Brown, T. M. 2001b, "STIS CCD Read Noise During Side-2 Operations", *Instrument Science Report* STIS 2001-05 (Baltimore: STScI)